

Fast-fluorescence dynamics in nonratiometric calcium indicators

M. Gersbach,¹ D. L. Boiko,^{2,*} C. Niclass,¹ C. C. H. Petersen,¹ and E. Charbon¹

¹Ecole Polytechnique Fédérale de Lausanne, Quantum Architecture Group, 1015, Lausanne, Switzerland

²Centre Suisse d'Electronique et de Microtechnique SA, 2002, Neuchâtel, Switzerland

*Corresponding author: dmitri.boiko@csem.ch

Received September 4, 2008; revised November 10, 2008; accepted November 25, 2008;
posted December 4, 2008 (Doc. ID 101111); published January 30, 2009

The fluorescence decay of high-affinity nonratiometric Ca^{2+} indicator Oregon Green BAPTA-1 (OGB-1) is analyzed with unprecedented temporal resolution in the two-photon excitation regime. A triple exponential decay is shown to best fit the fluorescence dynamics of OGB-1. We provide a model for accurate measurements of the free Ca^{2+} concentration and dissociation constants of nonratiometric calcium indicators.

© 2009 Optical Society of America

OCIS codes: 170.6280, 160.2540, 260.2510, 170.2520, 300.6280, 180.2520.

Fluorescence lifetime imaging microscopy (FLIM) is used to locally probe the chemical environment of fluorophores, e.g., ion concentration, pH, or oxygen content [1,2]. To acquire time-resolved fluorescence images, the technique of time-correlated single-photon counting (TCSPC), in combination with detectors exhibiting single-photon sensitivity, is commonly used. This technique enables the measurement of photon time-of-arrival distributions with very high accuracies, independently of instabilities in the excitation beam intensity. So far, temporal resolutions of a few hundred picoseconds were considered sufficient in biomedical FLIM applications.

In this Letter, we analyze the fluorescence decay of the high-affinity Ca^{2+} indicator Oregon Green BAPTA-1 (OGB-1) under two-photon excitation conditions, using a TCSPC system of measured resolution 79 ps based on complementary metal-oxide semiconductor single-photon avalanche diode (SPAD) detector technology. Our measurements reveal a triple-exponential decay of OGB-1 fluorescence, which we show enables accurate measurements of Ca^{2+} concentration and dissociation constants of nonratiometric fluorescent probes. We provide a comparison with previously reported data [1,3,4].

The SPAD-based TCSPC system is depicted in Fig. 1. Our SPADs [5] are integrated in a 32×32 array and incorporate on-chip high-bandwidth input/output circuitry. The active region of a SPAD pixel [Fig. 1(b)] consists of a p^+n junction operating in Geiger mode. Owing to a small diameter ($7 \mu\text{m}$), SPADs show an extremely low dark-count rate (<10 Hz at room temperature). The photon-detection probability is 25% at 500 nm wavelength; the dead time is 25 ns with negligible afterpulsing ($<0.1\%$) [5].

Fluorescent molecules are excited in the two-photon regime [6] using a mode-locked Ti:sapphire laser (MaiTai, Spectra Physics) emitting 100 fs optical pulses at 800 nm wavelength [Fig. 1(a)]. The attenuated beam with an average power of 9 mW is focused on a sample using a $20\times$ microscope objective (XLUMPlanFL, Olympus), which also serves to collect the fluorescent emission. Fluorescence from

OGB-1 samples is directed toward the SPAD by a dichroic beam splitter (DBS) and a filter (E650SP, Chroma Technology) for suppression of backscattered excitation pulses. Another $20\times$ objective images the emission spot onto the SPAD. The low fluorescence

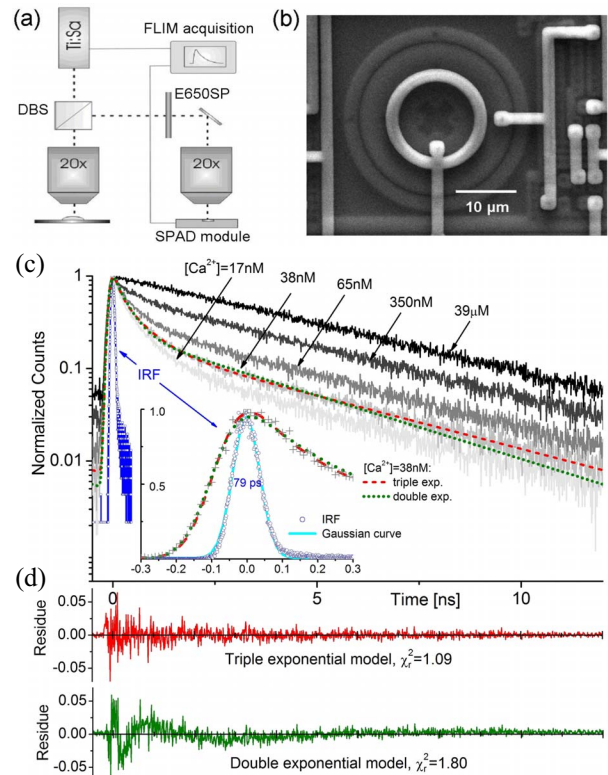


Fig. 1. (Color online) (a) Schematic of the experimental setup for fluorescence lifetime measurements. (b) Scanning electron microscope image of a SPAD. (c) Measured fluorescence decay of OGB-1 at various calcium concentrations (gray curves) and hyper-Rayleigh scattering from colloidal gold particles (open circles). For a 38 nM free Ca^{2+} concentration buffer, the numerical fits of the double-exponential (dotted curve, $\chi_r^2=1.80$) and triple-exponential (dashed curve, $\chi_r^2=1.09$) decay models are indicated. The inset shows a close-up of the initial interval of 600 ps width, and (d) shows the residues for the two models.

yield of the two-photon excitation results in a count rate at the detector of 10 kHz for an 80 MHz repetition rate of excitation pulses. Time discrimination is performed in a “reversed start–stop” configuration using a 6 GHz bandwidth oscilloscope (WaveMaster, LeCroy) incorporating a time-to-digital converter.

Figure 1(c) shows the instrument response function (IRF) of the entire system at 400 nm wavelength, recorded by measuring the hyper-Rayleigh scattering of 800 nm wavelength pulses in a solution of colloidal gold particles (G1652, Sigma-Aldrich) [7]. At the incident power of 90 mW, the average count rate of the detector is just 600 Hz. The measured response time jitter is 79 ps (FWHM). The IRF is only slightly asymmetrical and assumes a Gaussian-curve approximation $\text{IRF} = \exp(-t^2/2\sigma_{\text{IRF}}^2)$ (inset).

Fluorescent samples were composed of 2 μl OGB-1 dye (O6806, Molecular probes) and 20 μl Ca:EGTA buffer solutions from the calibration kit (C3008MP, Molecular Probes) with quoted free Ca^{2+} concentrations in the range of 17 nM to 39 μM . Several fluorescence decay curves measured in the two-photon excitation regime are shown in Fig. 1(c). The fluorescence lifetimes were obtained from the numerical analysis of these data.

Thorough numerical fit must take into account the IRF of the system [4]. As opposed to conventional systems with strongly asymmetric IRF, the Gaussian-like IRF of our system assumes a simple analytical expression for the measured fluorescence decay. For a train of excitation pulses of period T , each term of a multiexponential decay process reads

$$I_k = \frac{1}{2} \left[\frac{1 + e^{-T/\tau_k}}{1 - e^{-T/\tau_k}} - \text{erf} \left(\frac{\sigma_{\text{IRF}}}{\sqrt{2}\tau_k} - \frac{t}{\sqrt{2}\sigma_{\text{IRF}}} \right) \right] \times \exp \left(-\frac{t}{\tau_k} + \frac{\sigma_{\text{IRF}}^2}{2\tau_k^2} \right), \quad k = \{f, i, s\}, \quad (1)$$

where a triple-exponential decay is assumed and index k indicates fast (f), intermediate (i) and slow (s) temporal components; τ_k is the fluorescence emission lifetime ($\tau_f < \tau_i < \tau_s$); and $\text{erf}(z) = 2/\sqrt{\pi} \int_0^z \exp(-\xi^2) d\xi$ is the error function. Equation (1) takes the periodic train of excitation pulses and response time jitter of the SPAD into account, such that our data in Fig. 1 do not require deconvolution processing.

Analysis of the OGB-1 fluorescence reveals the best agreement with a triple-exponential decay approximation. The data are modeled using the function $A_f I_f + A_i I_i + (1 - A_f - A_i) I_s$, with the fast $I_f(t)$, intermediate $I_i(t)$, and slow $I_s(t)$ decaying components [Eq. (1)] of normalized partial intensities A_f , A_i , and $A_s = 1 - A_f - A_i$, respectively. Figure 1(c) details a comparison between the double-exponential (dotted curve) and triple-exponential (dashed curve) models applied to fluorescence from a 38 nM Ca^{2+} concentration sample. The residues [Fig. 1(d)] do not show any bias that might be caused by the Gaussian curve approximation of the IRF, while the quality of the numerical fit is improved in case of the triple-exponential model, as also confirmed by the reduced χ^2 values.

Wilms *et al.* [5] made the same observation for OGB-1 fluorescence in the absence of Ca^{2+} . However, it was attributed to contaminating dye derivatives. Previously reported data [1,3,4] for OGB-1 fluorescence lifetimes thus assume double-exponential decay. We argue that at high Ca^{2+} concentration, large amplitude of long-leaving component make it difficult to resolve short-lifetime components with small amplitudes, and the FLIM systems used in [1,3,4] exhibit insufficient temporal resolution.

Using triple-exponential fluorescence decay [Eq. (1)] with the lifetimes independent of the calcium buffer [1,4], we applied a global numerical analysis to our data, yielding the partial intensities A_k in function of free Ca^{2+} concentration and the lifetimes τ_k (Fig. 2). Temporal resolution of our system allows the short-lifetime component ($\tau_f \sim 188 \pm 6$ ps) to be unambiguously resolved in the background of the intermediate- and long-living fluorescence ($\tau_i \sim 768 \pm 16$ ps and $\tau_s \sim 4.18 \pm 0.01$ ns). The partial intensities A_f and A_i decrease, while the slow-component intensity $A_s = 1 - A_f - A_i$ increases with concentration [Ca^{2+}].

We attribute the short- and long-lifetime components to, respectively, unbound and Ca^{2+} -bound OGB-1 with a simple 1:1 complex stoichiometry. As

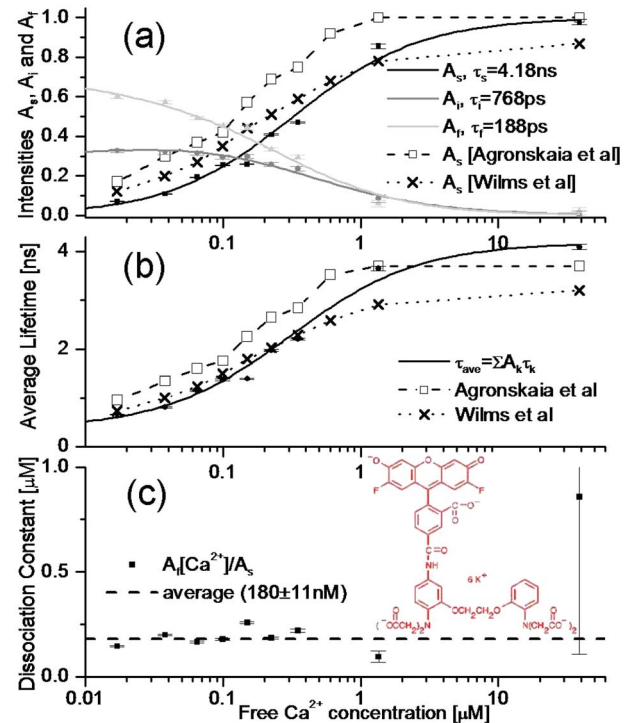


Fig. 2. (Color online) (a) Partial intensities A_s , A_i , and A_f of the slow ($\tau_s = 4.18 \pm 0.01$ ns), intermediate ($\tau_i = 768 \pm 16$ ps), and fast ($\tau_f = 188 \pm 6$ ps) decay components and (b) the mean lifetime $\tau_{\text{ave}} = \sum_k A_k \tau_k$ of OGB-1 fluorescence as a function of the free Ca^{2+} concentration in comparison with the data from [3] and [4], $\chi_r^2 = 0.96$. The numerical fit to the model [Eq. (2)] (curves) yields $K_D = 195 \pm 9$ nM, $K_{Dn} = 4 \pm 6$ μM , and $n = 9 \pm 3$. (c) Ratio $A_f[\text{Ca}^{2+}]/A_s$ (points) and its variance-weighted mean, yielding $K_D = 180 \pm 11$ nM (dashed line). The inset shows the structure of OGB-1 molecule.

such, and because the intensities are defined by complex concentrations, we obtain that $A_f \propto [D]$ and $A_s \propto [\text{CaD}] = K_D^{-1}[\text{Ca}^{2+}][D]$, with $[D]$ and $[\text{CaD}]$ being the unbound and Ca-bound OGB-1 concentrations and K_D the dissociation constant of the 1:1 complex. The ratio $A_f[\text{Ca}^{2+}]/A_s$ thus yields an estimate of the dissociation constant. In Fig. 2(c), a weighted-average ratio 180 ± 11 nM is in good agreement with the quoted (by manufacturer) K_D of 170 nM.

In Fig. 2, the long-lifetime component A_s is in good agreement with the measurements of Agronskaia *et al.* [3] and Wilms *et al.* [4], but in [4], $A_s < 1$ in Ca^{2+} -saturated buffer and K_D is too high (~ 300 nM). These discrepancies are attributed to the dye impurities and to the difference in two-photon absorption cross sections of Ca-bound and unbound OGB-1, which are said to be too difficult to be quantified [4].

For the Ca-bound OGB-1, Lakowicz [1] reported τ_s of 4 ns, which agrees well with our data. In [3], τ_s varies in the range 2.6–3.7 ns, while in [4], $\tau_s = 3.63$ ns. For the Ca-free OGB-1, a single-lifetime component τ_f has been measured of 700 [1], 290–420 [3], and 346 ps [4], respectively. These results correspond to the combined effect of the decay processes with the lifetimes $\tau_f \sim 190$ ps and $\tau_i \sim 770$ ps in our measurements, which may not have been resolved in previous studies. The experimental setup in [4] relies on a commercially available photomultiplying tube with a quoted timing jitter of 200 ps. Other data [1,3] are reported without the timing resolution.

Owing to the Ca-binding features of the octadentate chelator BAPTA [8], the 1:1 stoichiometry is usually attributed to the Ca-bound OGB-1 as well. However, the molecule of OGB-1 has an asymmetric structure with respect to its BAPTA moiety (Fig. 2, inset). The asymmetric arrangement of the carboxyl functional groups, benzol rings, fluorine, and nitrogen atoms as well as the variations of electronic density from low (at hydrogen in carboxyl groups) to high (at benzol rings, F and O atoms) assume a polarity of the molecule and, as a consequence, weak dipole-dipole intermolecular forces. As a result of such interaction forces, several OGB-1 molecules might be coordinated to a Ca-bound OGB-1 thus forming a polymolecular association with a calcium:indicator molar ratio 1: n . The intermediate lifetime component τ_i in Fig. 2 then might be attributed to such polymolecular association, yielding $A_i \propto [\text{Ca}_{1/n}\text{D}] = K_{Dn}^{-1/n}[\text{D}] \times [\text{Ca}^{2+}]^{1/n}$, with K_{Dn} being the corresponding dissociation constant. Note that formation of a polymolecular structure is a very complex processes and requires thorough investigations, but a non-1:1 stoichiometry of Ca:OGB-1 has been reported in [9]; here it allows us to build an accurate model:

$$\frac{[\text{Ca}^{2+}]}{K_D} = \frac{A_s}{A_f} = \frac{A_s}{1 - A_s} \left[1 + \frac{A_i}{A_f} \right], \quad \frac{[\text{Ca}^{2+}]}{K_{Dn}} = \left(\frac{A_i}{A_f} \right)^n. \quad (2)$$

In the limit $K_{Dn} \rightarrow \infty$ (double-exponential decay), it agrees with the Hill equation, as opposed to the

model in [4]. The numerical fit of data in Fig. 2 reports small binding affinity ($K_{Dn} \sim 4 \mu\text{M}$) and $n=9$, indicating the most probable form of polymolecular association with eight Ca-free molecules coordinated to the Ca-bound OGB-1. The dissociation constant K_D reported by the fit is 195 nM, in agreement with the average of $A_f[\text{Ca}^{2+}]/A_s$ (bottom panel).

The triple-exponential fluorescence decay in nonratiometric Ca probes as a result of dye contaminations was suggested by Lakowicz *et al.* [10] for the Calcium Green (CG-1). The CG-1 molecule has the same structure as OGB-1, but the two F atoms are replaced by Cl, yielding [10] $\tau_f = 50$ ps, $\tau_i = 450$ ps, and $\tau_s = 3.7$ ns. Interestingly, the signature of non-1:1 stoichiometry has been noticed for Ca-bound CG as well [11]. We find that at low Ca^{2+} concentration, the ratio $A_f[\text{Ca}^{2+}]/A_s$ in [10] is a constant of 170 ± 20 nM, yielding K_D close to the quoted value of 190 nM. At high Ca concentration, the bandpass of the system (2 GHz modulation using a frequency-domain FLIM technique) was insufficient to accurately measure the small component A_f . The data in [10] can thus be accurately interpreted in the framework of our model [Eq. (2)] without appealing to dye impurities. (K_D obtained in [10] using a conventional model [12] is 128 nM).

In summary, we have shown that high-temporal resolution measurements of the triple-exponential fluorescence decay of nonratiometric Ca^{2+} indicators allow the free Ca^{2+} concentration and dye dissociation constant to be measured precisely.

D. L. B. is grateful to Leonid Zekel and Edwin Constable for discussions on the model. This research was supported by a grant of the Swiss National Science Foundation and by Centre des Systèmes Intégrés of Ecole Polytechnique Fédérale de Lausanne.

References

1. J. Lakowicz, *Principles of Fluorescence Spectroscopy* (Plenum, 1999).
2. K. Suhling, P. M. W. French, and D. Phillips, *Photochem. Photobiol. Sci.* **4**, 13 (2005).
3. A. V. Agronskaia, L. Tertoolen, and H. C. Gerritsen, *J. Biomed. Opt.* **9**, 1230 (2004).
4. C. D. Wilms, H. Schmidt, and J. Eilers, *Cell Calcium* **40**, 73 (2006).
5. C. Niclass, A. Rochas, P. A. Besse, and E. Charbon, *IEEE J. Solid-State Circuits* **40**, 1847 (2005).
6. W. Denk, J. H. Strickler, and W. W. Webb, *Science* **248**, 73 (1990).
7. A. Habenicht, J. Hjelm, E. Mukhtar, F. Bergstrom, and L. B. A. Johansson, *Chem. Phys. Lett.* **354**, 367 (2002).
8. R. Y. Tsien, *Biochemistry* **19**, 2396 (1980).
9. D. Thomas, S. C. Tovey, T. J. Collins, M. D. Bootman, M. J. Berridge, and P. Lipp, *Cell Calcium* **28**, 213 (2000).
10. J. R. Lakowicz, H. Szmajnski, and M. L. Johnson, *J. Fluoresc.* **2**, 47 (1992).
11. M. Eberhard and P. Erne, *Biochem. Biophys. Res. Commun.* **180**, 209 (1991).
12. G. Grynkiewicz, M. Poenie, and R. Y. Tsien, *J. Biol. Chem.* **260**, 3440 (1985).